

HNPS Advances in Nuclear Physics

Vol 10 (1999)

HNPS1999



The exotic $\mu^- \rightarrow e^-$ conversion in Nuclei: An Interplay of Atomic, Nuclear and Particle Physics.

T. S. Kosmas

doi: [10.12681/hnps.2180](https://doi.org/10.12681/hnps.2180)

To cite this article:

Kosmas, T. S. (2019). The exotic $\mu^- \rightarrow e^-$ conversion in Nuclei: An Interplay of Atomic, Nuclear and Particle Physics. *HNPS Advances in Nuclear Physics*, 10, 120–131. <https://doi.org/10.12681/hnps.2180>

The exotic $\mu^- \rightarrow e^-$ conversion in Nuclei: An Interplay of Atomic, Nuclear and Particle Physics.

T.S. Kosmas

Theoretical Physics Division, University of Ioannina, GR-45110 Ioannina, Greece.

Abstract

The partial rates of all kinematically accessible channels (for coherent and incoherent processes) of the exotic $\mu^- \rightarrow e^-$ conversion in the currently interesting nuclei ^{27}Al , ^{48}Ti , and ^{208}Pb are investigated. The assumed muon-number violation involves exchange of various particles in conventional extensions of the standard model and in minimal supersymmetric models with R-parity conserving and R-parity violating interactions. The transition matrix elements obtained are used to extract very severe constraints for the flavor violation parameters entering the effective Lagrangians resulting in the framework of specific particle models.

1 Introduction

The anomalous conversion of a bound negative muon (μ_b^-) to an electron,

$$(A, Z) + \mu_b^- \rightarrow e^- + (A, Z)^*, \quad (1)$$

is a lepton flavor violating process predicted to occur in a plethora of new-physics extensions of the standard model [1–5]. In addition, experimentally it is accessible with incomparable sensitivity, a feature which has established it as one of the best probes to search for lepton flavor violation beyond the standard model.

Recently, in view of the indications for neutrino oscillations in super-Kamiokande and LSND data, new hope has revived among the experimentalists of nuclear and particle physics to detect other signals for physics beyond the standard model. The fact that the upper limits of the branching ratio of the $\mu^- \rightarrow e^-$ conversion relative to the ordinary muon capture, $R_{\mu e} = \Gamma(\mu^- \rightarrow e^-)/\Gamma(\mu^- \rightarrow \nu_\mu)$, offer the lowest constraints compared to any purely leptonic rare process motivated a new $\mu^- \rightarrow e^-$ conversion experiment, the so called MECO experiment at Brookhaven [6–8], which

got recently scientific approval and is planned to start soon. The MECO experiment is going to use a new very intense μ^- beam and a new detector operating at the Alternating Gradient Synchrotron (AGS). The basic feature of this experiment is the use of a pulsed μ^- beam to significantly reduce the prompted background from π^- and e^- contaminations. For technical reasons the MECO target has been chosen to be the light nucleus ^{27}Al .

Traditionally the $\mu-e$ conversion process was searched by employing medium heavy (like ^{48}Ti and ^{63}Cu) [9] or very heavy (like ^{208}Pb and ^{197}Au) [10,11] targets (for a historical review on such experiments see Ref. [12]). The best upper limits on $R_{\mu e}$ set up to the present have been extracted at PSI by the SINDRUM II experiments resulting in the values

$$R_{\mu e}^{Ti} < 6.1 \times 10^{-13} \quad [9], \quad R_{\mu e}^{Pb} < 4.6 \times 10^{-11} \quad [10].$$

The experimental sensitivity of the Brookhaven experiment on ^{27}Al will be roughly 2×10^{-17} [7,8], i.e. three to four orders of magnitude below the existing experimental limits.

The purpose of this work is to offer theoretical support primarily for the Brookhaven experiment by investigating state-by-state all the accessible $\mu^- \rightarrow e^-$ conversion channels for the MECO target. To this aim we performed a full s-d shell-model calculation for the transition matrix elements of the relevant $\mu^- \rightarrow e^-$ operators [6,13–16]. Furthermore, we use these matrix elements and the sensitivity of the MECO experiment to constrain the values of the parameters of several extensions of the standard model which exhibit the process (1). These parameters are involved in lepton flavor violating Lagrangians predicting this exotic process (e.g. couplings of scalar, vector etc. current components, neutrino mixing angles and masses, supersymmetric couplings etc.). The above limits are compared with those resulting from other experiments [9,10].

2 The particle- and nuclear-physics background of $\mu^- \rightarrow e^-$ conversion

On the theoretical side, it is well known that process (1) is a very good example of the interplay between particle and nuclear physics. From the underlying particle physics point of view, the family lepton quantum numbers L_e , L_μ , L_τ are conserved within the standard model (SM) in all orders of perturbation theory but this is an accidental consequence of the SM field content and gauge invariance. Processes like the $\mu-e$ conversion, which violates the muon and electron quantum-number conservation, play an important role in the study of flavor-changing neutral currents. Nowadays, there are many mechanisms beyond the standard model leading to the $\mu-e$ conversion [1–5]. They are mediated by various particles, like virtual photons, W -boson or Z -particle exchange [1,3,4], exotic particles like Higgs scalars etc. [2,4], supersymmetric particles (squarks, sleptons, gauginos, higgsinos etc.) with and without involving R -parity violation [12,17,18]. Some Feynman diagrams are

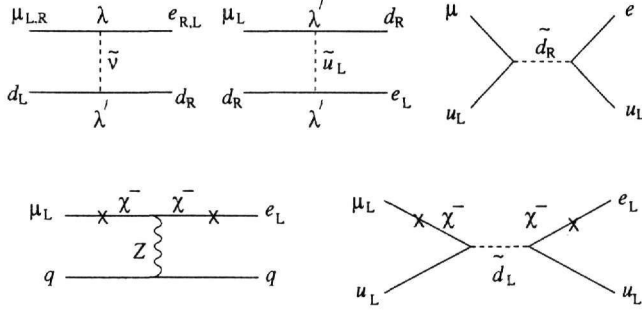


Fig. 1. Photonic and nonphotonic mechanisms exhibiting the $\mu^- \rightarrow e^-$ process within the context of conventional extensions of the standard model (a-c), as well as supersymmetric theories (d,e). The hadronic vertex is mediated by photon exchange (a,d), Z -particle exchange (a,b,d,e), and W -boson exchange (c).

shown in Fig. 1 (one-loop-level diagrams) and Ref. [18] (tree-level diagrams). In Fig. 1 mixing of intermediate neutrinos (ν_i) including possible heavy species (N_i) and gauge bosons or mixing of sleptons (l_i) in supersymmetric models with R -parity conservation is involved. The lepton-flavor violation in the case of R -parity violating diagrams of Fig. 2 is mediated by the exchange of Z bosons, sneutrinos $\tilde{\nu}$, up \tilde{u}_L and down \tilde{d}_R squarks as explained in Ref. [18]. The effective $\mu^- \rightarrow e^-$ conversion Lagrangian in the above new-physics extensions of the standard model is given by means of a set of lepton-flavor-violating parameters. In the context of these models the (μ^-, e^-) conversion operators are constructed first at nucleon and then at nuclear level by writing down the hadronic and leptonic currents. The aim of the nuclear physics calculations is to provide us with the necessary nuclear transition matrix elements of these operators which are essential to constrain the family lepton violating parameters by making use of the existing experimental limits or the expected sensitivity of ongoing experiments.

For the mechanisms involving vector and axial-vector interactions in the effective Hamiltonian density the hadronic current at nucleon level, needed for the nuclear-physics aspects of the process can be parametrized in a general manner as [1–3,17]

$$J^\mu = \bar{N} \gamma^\mu \left[(\beta_V^0 + \beta_V^1 \tau_3) + (\beta_A^0 + \beta_A^1 \tau_3) \gamma_5 \right] N, \quad (2)$$

where the coefficients β_V^τ , for the vector, and β_A^τ , for the axial vector, contain the corresponding couplings for isoscalar ($\tau = 0$) and isovector ($\tau = 1$) components, respectively. In models where the $\mu - e$ conversion occurs due to the exchange of scalar particles like exotic Higgs scalars etc., the hadronic current can be parametrized accordingly as

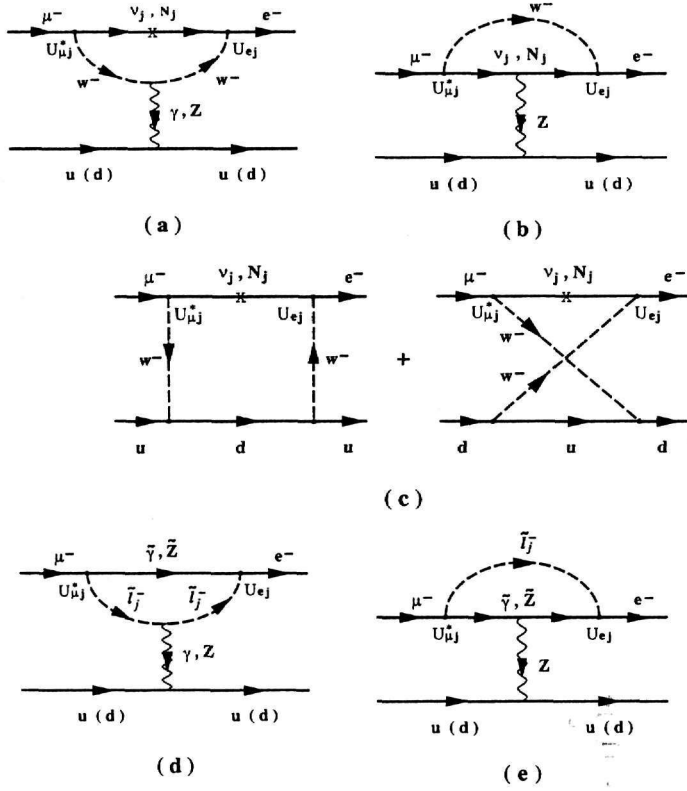


Fig. 2. Leading R-parity violating diagrams contributing to $\mu - e$ conversion at tree-level. (i) (upper diagrams): Trilinear terms mediated by the sneutrino $\tilde{\nu}$, up \tilde{u}_L and down \tilde{d}_R squarks in the intermediate states. (ii) (lower diagrams): Bilinear terms mediated via the chargino-lepton mixing (schematically denoted by crosses (X) on the lepton lines). The intermediate states of the diagrams are Z -bosons and squarks \tilde{d}_L .

$$J = \bar{N} \left[(\beta_S^0 + \beta_S^1 \tau_3) + (\beta_P^0 + \beta_P^1 \tau_3) \gamma_5 \right] N, \quad (3)$$

where now β_α^τ , $\alpha = S, P$ involve the corresponding couplings for the scalar (S) and pseudoscalar (P) components, respectively. Apparently, the values of the parameters β_α^τ with $\alpha = V, A, S, P$ and $\tau = 0, 1$ of Eqs. (2) and (3), depend on the specific elementary model assumed for the $\mu - e$ conversion. Some special cases are discussed in Refs. [4,18,21] and used in our previous works [6,18–22].

The Hamiltonians of Eqs. (2) and (3) give rise to both coherent and incoherent $\mu - e$ conversion channels. For the class of models where the coupling β_V^0 is not very small the coherent process, i.e. when the nucleus remains in its ground state,

dominates the rate [12,19]. Equation (2) shows that for the vector and axial vector currents the branching ratio $R_{\mu e^-}$, which is one of the most interesting quantities of the $\mu^- \rightarrow e^-$ process both theoretically and experimentally, can be expressed phenomenologically as a sum of isoscalar and isovector terms, arising from different couplings of the up and down quark. This holds also for the scalar and pseudoscalar current, see Eq. (3), in models where the structure of the corresponding nuclear current (ignoring the tensor components) is similar to that of the vector current but with different strength parameters $\beta_S^{0,1}$ [2,18].

The expression for the transition rate $\Gamma(\mu \rightarrow e^-)$ under some reasonable assumptions [2,4] is written in terms of the matrix element

$$\mathcal{M}_{V-A}^2 = |\beta_V^0 \mathcal{M}_V^{(0)} + \beta_V^1 \mathcal{M}_V^{(1)}|^2 + |\beta_A^0 \mathcal{M}_A^{(0)} + \beta_A^1 \mathcal{M}_A^{(1)}|^2 \quad (4)$$

for the current of Eq. (2), and

$$\mathcal{M}_{S-P}^2 = |\beta_S^0 \mathcal{M}_S^{(0)} + \beta_S^1 \mathcal{M}_S^{(1)}|^2 + |\beta_P^0 \mathcal{M}_P^{(0)} + \beta_P^1 \mathcal{M}_P^{(1)}|^2 \quad (5)$$

for the current of Eq. (3). Usually, the rates for the $\mu-e$ conversion are calculated by neglecting the lower component of the nucleon spinor (non-relativistic approximation). Then, the transition matrix elements $\mathcal{M}_\alpha^{(\tau)}$ entering Eqs. (4) and (5), which are referred to as the muon-nucleus overlap integrals, are written as

$$\mathcal{M}_\alpha^{(0)} = \langle \mathbf{f} | \sum_{j=1}^A \theta_j^\alpha e^{-i\mathbf{q} \cdot \mathbf{r}_j} \Phi_\mu(\mathbf{r}_j) | \mathbf{i} \rangle, \quad (6)$$

$$\mathcal{M}_\alpha^{(1)} = \langle \mathbf{f} | \sum_{j=1}^A \theta_j^\alpha \tau_{3j} e^{-i\mathbf{q} \cdot \mathbf{r}_j} \Phi_\mu(\mathbf{r}_j) | \mathbf{i} \rangle, \quad (7)$$

where the index j runs over all nucleons of the nucleus and \mathbf{q} is the momentum transfer, $\Phi_\mu(\mathbf{r}_j)$ denotes the upper component of the muon spinor (the small lower component is neglected) and θ_j^α are given by

$$\theta_j^\alpha = \begin{cases} 1, & \alpha=S, V \quad (\text{scalar, vector components}) \\ \sigma_j, & \alpha=A \quad (\text{axial vector component}) \\ \sigma_j \cdot \hat{\mathbf{q}}, & \alpha=P \quad (\text{pseudoscalar component}) \end{cases} \quad (8)$$

For the ground-state-to-ground-state contributions $|\mathbf{f}\rangle = |\mathbf{i}\rangle \equiv |g.s.\rangle$. In the case of light nuclear targets ($A \leq 100$) the $\mu-e$ rates are calculated by factorizing out of the muon-nucleus overlap integrals of Eqs. (6) and (7) a mean value of the muon wavefunction (factorization approximation) as

$$\mathcal{M}_\alpha^{(\tau)} \approx \langle \Phi_\mu \rangle \langle \mathbf{f} | \Omega_\alpha^{(\tau)} | \mathbf{i} \rangle \equiv \langle \Phi_\mu \rangle M_\alpha^{(\tau)}, \quad \alpha = S, V, A, P \quad (9)$$

(see also Ref. [12]), where Ω_α^τ denotes any of the six operators of Eqs. (6) and (7). The latter approximation permits the separate calculation of the nuclear matrix elements M_α^τ . The radial part $\Phi_\mu(r)$ of the muon wavefunction can also be exactly obtained by solving numerically the Schrödinger (or Dirac) equation with the Coulomb potential [18] (see Sect. 4 below). This enables exact evaluation of the muon-nucleus overlap integrals of Eqs. (6) and (7).

In some extensions of the standard model the expression which gives the branching ratio $R_{\mu e^-}$, especially for the dominant coherent channel, can be separated in two parts, the one which contains the nuclear-structure dependence and the one involving the elementary-particle-sector parameters as

$$R_{\mu e^-} = \rho \gamma . \quad (10)$$

The quantity ρ is independent of nuclear physics [17] and contains the flavor-violating parameters which mainly describe the leptonic currents. Thus, e.g. for photon exchange, ρ contains the four electromagnetic form factors f_{E0} , f_{E1} , f_{M0} , f_{M1} parametrized in a specific elementary model [17] as

$$\rho = (4\pi\alpha)^2 \frac{|f_{M1} + f_{E0}|^2 + |f_{E1} + f_{M0}|^2}{(G_F m_\mu^2)^2} . \quad (11)$$

The function $\gamma(A, Z)$ of Eq. (10) contains the nuclear information through the matrix elements M^2 [4] as

$$\gamma(A, Z) \equiv \gamma = \frac{E_e q}{m_\mu^2} \frac{M^2}{G^2 Z f_{GP}(A, Z)} , \quad (12)$$

where E_e is the outgoing-electron energy and f_{GP} is the Primakoff function [23]. We should note that in Eq. (12) the mean muon wave function has been cancelled out by applying the factorization approximation for the μ^- -capture, i.e. in the denominator, too.

As it becomes obvious from the above, the $\mu - e$ conversion experiments could be sensitive to the scalar interactions too. In this work, we focus on the calculation of particle-model-independent nuclear matrix elements to be used in order to draw conclusions about the scalar contribution and extract constraints on the scalar couplings which have not been explicitly included in our previous works. We apply our formalism in two cases: (i) assuming that the muon number violation occurs due to the exchange of scalar Higgs particles and (ii) in the R-parity violating mechanisms of Ref. [18].

3 Nuclear matrix elements in the factorization approximation

The in this work performed state-by-state calculations refer to both coherent and incoherent processes and use the method we have formulated in our previous works [6,13]. The relevant $\mu-e$ conversion operators are adjusted to the odd-A ^{27}Al target employed by the Brookhaven experiment. We afterwards compare these results with those for the nuclei ^{48}Ti and ^{208}Pb , i.e. the targets of the SINDRUM II experiment [9,10], obtained with different methods.

For the coherent rate in light nuclei, like ^{27}Al , the factorization approximation of Eq. (9) is very good. Then the contributions of the vector- and scalar-current components in M_{coh} are

$$M_{V,S} = \beta_{V,S}^0(ZF_Z + NF_N) + \beta_{V,S}^1(ZF_Z - NF_N). \quad (13)$$

This means that they can be expressed in terms of the nuclear form factors $F_Z(q^2)$ (for protons) and $F_N(q^2)$ (for neutrons) defined as

$$F_Z = \frac{1}{Z} \sum_j \hat{j}(j \| j_0(qr) \| j) (V_j^p)^2, \quad (14)$$

$$F_N = \frac{1}{N} \sum_j \hat{j}(j \| j_0(qr) \| j) (V_j^n)^2. \quad (15)$$

These form factors are easily estimated (for this channel only the ground-state wave function of the studied nucleus is required) and contain the single-particle-orbit occupancies $(V_j)^2$ for the evaluation of which one must use in the proton-neutron representation a nuclear model as e.g. the QRPA (see calculations for ^{48}Ti and ^{208}Pb in Ref. [17]), shell-model (see calculations for ^{27}Al in Refs. [6,13]) etc.

In the general case the target nucleus of Eq. (1) is excited and then, in the nuclear matrix elements M^2 of Eq. (12), in addition to the $M_{V,S}^2$ part there is also a contribution coming from the axial-vector operators of Eqs. (6) and (7) (we neglect the small pseudoscalar term). In this case, all the matrix elements of the operators (6), (7) can be usually obtained via the corresponding multipole-expansion tensor operators $T_M^{(I,S)J}$ (J is the operator angular-momentum rank and M its projection) obtained by expanding the exponential $e^{i\mathbf{q}\cdot\mathbf{r}}$ [19] which for the spin independent component ($S=0$), Fermi type operator, and the spin dependent component ($S=1$), the Gamow-Teller-type operator, have been defined in Ref. [19]. In the factorization approximation, the matrix elements M^2 of Eq. (12) for the inclusive process are given by

$$S_{V,S} = \sum_{f,J} \left(\frac{q_f}{m_\mu} \right)^2 \left| \left(J_f \| T^{(J,0)J} \| J_i \right)_{V,S} \right|^2, \quad (16)$$

$$S_A = \sum_{f,J} \sum_{l=J,J\pm 1} \left(\frac{q_f}{m_\mu} \right)^2 \left| \left(J_f \| T^{(l,1)J} \| J_i \right)_A \right|^2, \quad (17)$$

where the values of J are restricted to $|J_i - J_f| \leq J \leq J_i + J_f$. For the odd-A nucleus ^{27}Al $J_i = (5/2)^+$. The reduced matrix elements of the multipole operators $T^{(l,S)J}$ appearing in Eqs. (16) and (17) are defined as

$$(f \| T^{(l,S)J} \| i)_\alpha = \sum_{j_1 j_2} m^{(l,S)J}(j_2 j_1) \left[\beta_\alpha^0 D(j_2 j_1; J, T = 0) + \beta_\alpha^1 D(j_2 j_1; J, T = 1) \right], \quad (18)$$

where $m^{(l,S)J}$ include the angular-momentum-coupling coefficients [19]. The coefficients β_α^r essentially select the specific (photonic, W -boson exchange, etc.) reaction mechanism and current component as we have stated before. The functions $D(jj'; J, T)$ are the one-body transition densities.

4 Results and Discussion.

For the reliability of the investigated $\mu - e$ conversion rates we first tested our method as follows. We have calculated the energy spectrum and the eigenvectors of the nucleus ^{27}Al in the full sd shell-model space in isospin formalism. We used Wildenthal's set of fitted, mass-dependent two-body matrix elements and single-particle energies, the so-called USD interaction [14], with the code OXBASH [16]. For each spin-isospin combination we calculated the first 1000 states reaching up to about 45 MeV in excitation energy. The low-energy spectrum of ^{27}Al is well reproduced, thus qualifying the structure of the states involved. The momentum transfer q involved in the matrix elements of Eqs. (6) and (7),

$$q \equiv |\mathbf{q}| = m_\mu - \epsilon_b - E_x, \quad (19)$$

with E_x being the excitation energy of the final nuclear state, is equal to $q = m_\mu - \epsilon_b = 0.53 \text{ fm}^{-1}$ for the coherent channel of ^{27}Al . The atomic 1s-muon binding energy is $\epsilon_b = 0.47 \text{ MeV}$ and $m_\mu = 105.6 \text{ MeV}$. For the values of q in the other nuclei discussed here see Table 1. The single-particle orbit occupancies $(V_j)^2$ needed to evaluate the nuclear form factors $F_Z(q^2)$ and $F_N(q^2)$ were evaluated by performing a shell-model calculation of the ^{27}Al ground state in the proton-neutron formalism too. The shell-model form factors found are in very good agreement (see Ref. [6]) with the experimental form factors obtained from electron scattering (for proton form factors) [24] or from pionic atom data (for neutron form factors) [25].

As it has been seen in Sect. 2, the pure transition-rate calculations needed for the $\mu - e$ conversion studies involve mainly the integrals of Eqs. (6) and (7). For the coherent process, in the case of ^{48}Ti and ^{208}Pb for which the factorization approximation is not very good, these integrals have been exactly calculated using

experimental proton densities ρ_p from Ref. [24] and neutron densities ρ_n from Ref. [25]. The results for $\mathcal{M}^{(0)}$ and $\mathcal{M}^{(1)}$ are shown in Table 1.

Table 1

Isoscalar and isovector transition matrix elements for the coherent $\mu - e$ process, i.e. muon-nucleus overlap integrals $\mathcal{M}_{V,S}^{(\tau)}$, $\tau = 0, 1$ of Eqs. (6) and (7). Other useful quantities (see text) are also included.

Nucleus	$ \mathbf{q} (fm^{-1})$	$\epsilon_b (MeV)$	$\mathcal{M}_{V,S}^{(0)} (fm^{-3/2})$	$\mathcal{M}_{V,S}^{(1)} (fm^{-3/2})$
^{27}Al	0.531	-0.470	0.046	0.001
^{48}Ti	0.529	-1.264	0.115	0.012
^{208}Pb	0.482	-10.516	0.490	0.076

The wave function of the muon at the atomic level was obtained by solving the Schrödinger equation using the Coulomb potential produced by the charge densities discussed before. The nucleon finite size was taken into consideration and vacuum polarization corrections were included as in Ref. [22]. In this way we constructed an analytical form for the muon wave function (given in terms of sigmoid functions) which was advantageous for our numerical integrations.

For explicit calculations of the incoherent transition matrix elements of Eqs. (16) and (17) one can combine the single-particle matrix elements of Ref. [19] with the one-body transition densities of OXBASH [15]. Our state-by-state calculations of the excited states show that the incoherent rate contributions in ^{27}Al are rather small. For $S_{V,S}$ the incoherent strength is concentrated in the first few excited states. For S_A the situation is different, but its contribution to the total strength is much smaller than that of the vector matrix elements S_V .

Table 2

Isoscalar and isovector contributions to the inclusive $\mu - e$ conversion rate in ^{27}Al , i.e. the matrix elements S_α^τ of Eqs. (16) and (17). These quantities do not depend on the specific elementary model assumed for the $\mu - e$ conversion (see text).

$S_{V,S}^{(0)}$	$S_{V,S}^{(1)}$	$S_A^{(0)}$	$S_A^{(1)}$
110.50	2.849	9.117	6.745

Table 2 shows the individual isoscalar ($S_\alpha^{(0)}$) and isovector ($S_\alpha^{(1)}$) matrix elements of Eqs. (16) and (17) for the inclusive $\mu - e$ conversion process in ^{27}Al . In practice these are obtained by setting either β_α^0 (for isoscalar contribution) or β_α^1 (for isovector contribution) to zero and dividing by the square of the non-zero model-dependent

Table 3

Upper limits on the elementary sector part of the exotic $\mu - e$ conversion branching ratio (quantity ρ of Eq. (11) and quantity \mathcal{Q} of Eq. (4)) extracted by using the sensitivity of the MECO experiment for the ^{27}Al target [7] and the recent experimental data for the nuclear targets ^{48}Ti and ^{208}Pb [10].

Mechanism	^{27}Al	^{48}Ti	^{208}Pb
Photonic	$\rho \leq 4.6 \times 10^{-18}$	$\rho \leq 7.1 \times 10^{-14}$	$\rho \leq 3.2 \times 10^{-12}$
W-boson exchange	$\rho \leq 5.8 \times 10^{-19}$	$\rho \leq 2.6 \times 10^{-14}$	$\rho \leq 1.1 \times 10^{-12}$
SUSY sleptons	$\rho \leq 1.8 \times 10^{-18}$	$\rho \leq 2.6 \times 10^{-14}$	$\rho \leq 1.1 \times 10^{-12}$
SUSY Z-exchange	$\rho \leq 7.3 \times 10^{-19}$	$\rho \leq 0.6 \times 10^{-14}$	$\rho \leq 0.2 \times 10^{-12}$
SUSY R-par. Viol.	$\mathcal{Q} \leq 5.10 \cdot 10^{-19}$	$\mathcal{Q} \leq 1.10 \cdot 10^{-14}$	$\mathcal{Q} \leq 2.27 \cdot 10^{-13}$

coefficient β_α^* . From Table 2 we see that the particle-model independent isoscalar matrix elements of the scalar and vector operators are much larger than those of the isovector ones. Thus, in the approximation of neglecting the isovector contribution one can constrain the isoscalar parameters β_α^0 . In general, the evaluation of the isoscalar ($\mathcal{M}_\alpha^{(0)}$) and isovector ($\mathcal{M}_\alpha^{(1)}$) transition matrix elements enables one to put bounds separately on the isoscalar and isovector parameters of the hadronic currents if, in the specific model, the $\mu^- \rightarrow e^-$ Hamiltonian is characterized by isoscalar or isovector dominance (see below).

The results of Tables 1 and 2 can be exploited for setting constraints on the parameters of a specific gauge model predicting the $\mu - e$ process. One can extract upper limits on the individual lepton flavor violation parameters (couplings of scalar, vector currents, neutrino masses etc. [1,4,17,18]) under certain assumptions. The most common assumption is the dominance of only one component of the $\mu - e$ conversion Lagrangian which is equivalent to constrain one parameter. In some cases we can write the branching ratio $R_{\mu e^-}$ as [2]

$$R_{\mu e^-} = \frac{G_F^2}{2\pi} \frac{q E_e [M_{V,S}^{(0)}]^2}{G^2 Z f_{GP}(A, Z)} \mathcal{Q}, \quad (20)$$

where

$$\mathcal{Q} \approx [\beta_V^0 + \beta_V^1 \mathcal{R}]^2 + [\beta_S^0 + \beta_S^1 \mathcal{R}]^2,$$

with $\mathcal{R} = M^{(1)}/M^{(0)}$ being the ratio of the isovector to isoscalar matrix elements. In general, especially for light nuclei, \mathcal{R} is very small. As an example see the case of R-parity violating SUSY mechanisms in Ref. [18].

In Table 3 we quote the upper bounds for the quantities ρ and \mathcal{Q} derived by using the expected experimental sensitivity of the Brookhaven experiment, $R_{\mu e^-} < 2 \times 10^{-17}$

for ^{27}Al and the recent experimental data on the branching ratio $R_{\mu e^-}$ for ^{48}Ti and ^{208}Pb given in the introduction. The limits of ρ and Q for the ^{27}Al target quoted in Table 3 improve by about four orders of magnitude over the previous ones. Using the upper limits for Q given in this table we can derive, by assuming isoscalar dominance, constraints on the scalar current couplings β_S^0 . In the R -parity violating Lagrangian for the ^{27}Al target [6,13] we obtain $|\beta_S^0| < 7 \times 10^{-10}$. The limit for β_S^0 obtained with the data of Ti target [10] is $|\beta_S^0| < 1.1 \times 10^{-7}$, i.e. more than two orders of magnitude weaker than the limit of ^{27}Al .

We should mention that significantly better improvement on these limits is expected from the ongoing experiments at PSI [9]. The analysis of the data obtained with the last run of the SINDRUM II experiment on the ^{48}Ti target is expected to reduce the best upper limit in the value $R_{\mu e^-} = 1 - 2 \times 10^{-13}$ [9].

5 Summary and Conclusions.

The transition matrix elements of the flavor violating $\mu^- \rightarrow e^-$ conversion are of notable importance in computing accurately the corresponding rates for each accessible channel of this exotic process. Such calculations provide useful nuclear-physics inputs for the expected new data from the MECO and PSI experiments to put severe bounds on the muon-number-changing parameters (isoscalar couplings, etc.) determining the effective currents in various models that predict the exotic $\mu^- \rightarrow e^-$ process.

From the existing data on $R_{\mu e^-}$ in ^{48}Ti and ^{208}Pb and the expected sensitivity of the designed MECO experiment on ^{27}Al [7] we obtained stringent upper limits on the quantities ρ and Q introduced in Eqs. (11) and (20).

References

- [1] W.J. Marciano and A.I. Sanda, Phys. Rev. Lett. **38** (1977) 1512 ; Phys. Lett. B **67** (1977) 303.
- [2] T.P. Cheng and L.F. Li, Phys. Rev D **16** (1977) 1425 ; O. Shanker, Phys. Rev D **20** (1979) 1608.
- [3] J.D. Vergados, Phys. Reports **133** (1986) 1.
- [4] T.S. Kosmas, G.K. Leontaris and J.D. Vergados, Prog. Part. Nucl. Phys. **33** (1994) 397.
- [5] P. Depommier and C. Leroy, Rep. Prog. Phys. **58** (1995) 61.
- [6] T. Siiskonen, J. Suhonen, and T.S. Kosmas, Phys. Rev. C **60** (Rapid Communication) (1999) 62501.

- [7] W. Molzon, The MECO Experiment: A search for $\mu^- N \rightarrow e^- N$ with sensitivity below 10^{-16} , Invited talk at Int. Conf. on "Symmetries in Physics at Intermediate and High Energies and Applications", Ioannina-Greece, Sept. 30 - Oct. 5, 1998.
- [8] W. Molzon, The improved tests of muon and electron flavor symmetry in muon processes, Spring. Trac. Mod. Phys. **163** (2000)
- [9] SINDRUM II Collaboration, A. van der Schaaf, Phys. Rev. C, submitted and Private Communication.
- [10] SINDRUM II Collaboration, C. Dohmen *et al.*, Phys. Lett. B **317** (1993) 631 ; W. Honecker *et al.*, Phys. Rev. Lett. **76** (1996) 200.
- [11] TRIUMF Collaboration, S. Ahmad *et. al.*, Phys. Rev. Lett. **59** (1987) 970 ; Phys. Rev. D **38** (1988) 2102.
- [12] T.S. Kosmas, J.D. Vergados, and A. Faessler, Phys. Atom. Nucl. **61** (1998) 1261.
- [13] T. Siiskonen, T.S. Kosmas, and J. Suhonen, Phys. Rev. C, to be submitted
- [14] B.H. Wildenthal, Prog. Part. Nucl. Phys. **11** (1984) 5.
- [15] R.B. Firestone, V.S. Shirley, S.Y.F. Chu, C.M. Baglin, and J. Zipkin, *Table of Isotopes CD-ROM*, Eighth Edition, Version 1.0 (Wiley-Interscience, New York, 1996).
- [16] B.A. Brown, A. Etchegoyen, and W.D.M. Rae, The computer code OXBASH, MSU-NSCL report (1988) 524.
- [17] T.S. Kosmas, A. Faessler, and J.D. Vergados, J. Phys. G **23** (1997) 693.
- [18] A. Faessler, T.S. Kosmas, S. Kovalenko, and J.D. Vergados, hep-ph/9904335; T.S. Kosmas and S. Kovalenko, Phys. Atom. Nucl., in press.
- [19] T.S. Kosmas, J.D. Vergados, O. Civitare and A. Faessler, Nucl. Phys..A **470** (1994) 397 ; T.S. Kosmas, Z. Ren and A. Faessler, Nucl. Phys. A, in press.
- [20] J. Schwieger, T.S. Kosmas, and A. Faessler, Phys. Lett. B **443** (1998) 7.
- [21] T.S. Kosmas, A. Faessler, F. Šimkovic, and J.D. Vergados, Phys. Rev. C **56** (1997) 526.
- [22] H.C. Chiang, E. Oset, T.S. Kosmas, A. Faessler and J.D. Vergados, Nucl. Phys. A **559** (1993) 526.
- [23] B. Goulard and H. Primakoff, Phys. Rev. C **10** (1974) 2034 ; T. Suzuki, *et al.*, Phys. Rev. C **35** (1987) 2212.
- [24] H. de Vries, C.W. de Jager, and C. de Vries, Atomic Data and Nuclear Data Tables **36** (1987) 495.
- [25] W.R. Gibbs and B.F. Gibson, Ann. Rev. Nucl. Part. Sci. **37** (1987) 411.